



Article

Ecological Policies Dominated the Ecological Restoration over the Core Regions of Kubuqi Desert in Recent Decades

Min Ren ¹, Wenjiang Chen ¹ and Haibo Wang ^{2,*}

¹ Center for Studies of Ethnic Minorities in Northwest China, School of History and Culture, Lanzhou University, Lanzhou 730000, China

² Key Laboratory of Remote Sensing of Gansu Province, Heihe Remote Sensing Experimental Research Station, Northwest Institute of Eco-Environment and Resources, Chinese Academy of Sciences, Lanzhou 730000, China

* Correspondence: whb@lzb.ac.cn; Tel.: +86-931-4967972

Abstract: Climate change and human activities significantly affected environmental changes in drylands. However, the relative roles remain unclear regarding these factors' effects on environment changes in drylands. Herein, we analyzed vegetation change trends using remote-sensing datasets to determine the interactions of vegetation, climate, and anthropogenic activities in an arid region of China, Kubuqi Desert. Our study showed that 67.64% of the pixels of fractional vegetation coverage (FVC) increased in 2020 in comparison with those of 1986. The FVC exhibited a significant greening trend (0.0011/yr, $p < 0.05$) in 1986–2020 as a whole. This greening trend revealed two distinct periods separated by a turning point in 2001. There was no clear trend of FVC before 2001, and then there was a dramatically greening trend since 2001 in most regions of the study area. The increasing rate (0.0036/yr) in the later period was three times higher than the entire period. The accelerated increasing trend was due to the variable compound effects of climate and human activities. The correlation between FVC and precipitation was mainly positive, which outweighs the significantly negative correlation between vegetation and temperature. However, both climatic factors cannot well explain the trends of vegetation dynamics, implying a possible role for human activities. Generally, climate change and anthropogenic activities contributed 42.15% and 57.85% to the overall vegetation variations in 1986–2020. Specifically, the relative role of the two factors was vastly different in two distinct periods. Climate change led the dominant roles (58.68%) in the vegetation variations in 1986–2001, while anthropogenic activities dominated (86.79%) in driving vegetation recovery in the period after 2001. Due to the massive ecological conservation programs such as the Grain for Green Project launched in 2001, substantial deserts have been transformed into grasslands and forests. This analysis highlights the ecological policies largely responsible for vegetation restoration and provides references for ecological protection and sustainable development in eco-fragile ecosystems.



Citation: Ren, M.; Chen, W.; Wang, H. Ecological Policies Dominated the Ecological Restoration over the Core Regions of Kubuqi Desert in Recent Decades. *Remote Sens.* **2022**, *14*, 5243. <https://doi.org/10.3390/rs14205243>

Academic Editor: Izaya Numata

Received: 31 August 2022

Accepted: 15 October 2022

Published: 20 October 2022

Publisher's Note: MDPI stays neutral with regard to jurisdictional claims in published maps and institutional affiliations.

Keywords: drylands; NDVI; Hangjin Banner; grain for green program; vegetation change; anthropogenic activities; Google Earth Engine



Copyright: © 2022 by the authors. Licensee MDPI, Basel, Switzerland. This article is an open access article distributed under the terms and conditions of the Creative Commons Attribution (CC BY) license (<https://creativecommons.org/licenses/by/4.0/>).

1. Introduction

Drylands comprise about 41% of the global land surface [1] and play an important role in global terrestrial ecosystems [2,3]. However, these ecosystems are extremely fragile and tend to be desertified [4]. Land degradation or desertification occurs widely and is one of the most devastating socio-economic and environmental problems in drylands [5,6]. The occurrence and development of land desertification has caused a serious threat to eco-environment, economy development, and human welfare [7]. China, as one of the most severely desertified countries, experienced aeolian desertification dominating almost all dryland areas in northern China. Studies showed that the annual increasing rates of aeolian desertification were 1560 km²/yr from 1955 to 1975, 2100 km²/yr from 1976 to 1987,

and 3600 km²/yr from 1988 to 2000 [7], which resulted in a direct economic loss of about 54 billion RMB each year in China [8]. Therefore, the control and rehabilitation of desertified land is of great importance to the sustainable development of these regions [5]. The Chinese government has made a lot of efforts to maintain the stability of deserts and improve the qualities of the environment of dryland ecosystems over the past decades. Currently, combating desertification has achieved remarkable successes in China. However, although the expanding situation of desertification in most regions has been effectively prevented, certain desertified lands still continuously increased. In the above context, monitoring the spatiotemporal evolutionary characteristics and their responses to environmental changes were thus crucial to the conservation and restoration of the environment in desertified regions, as well as the social-economic sustainable development in eco-fragile drylands.

Vegetation, an important composition of dryland ecosystems, plays a critical role in preventing desertification and maintaining the security of ecological barriers to desertified lands [9]. Vegetation coverage (Fractional vegetation cover, FVC) is the ratio of the vertically projected area of vegetation to the total statistical area [8,10]; it reflects the status of vegetation growth and is widely used to describe regional eco-environmental qualities [11,12]. It is also an important indicator for revealing the developing process of desertification and plays an important role in climate change and terrestrial processes in drylands [13,14]. FVC has typically been estimated from the normalized difference vegetation index (NDVI) of completely covered vegetation (NDVI_v) and bare soil (NDVI_s). The remote-sensing-based NDVI is highly sensitive to the biophysical properties of vegetation, with the advantage of monitoring the spatiotemporal patterns of vegetation dynamics in large regions timely and effectively [11,15], which is widely used in monitoring the dynamics of FVC in dryland ecosystems [16].

Due to their water scarcity and sparse vegetation coverage, the structure and function of dryland environments are vulnerable to climate change and human activities [1,2]. Therefore, apparent spatiotemporal changes of vegetation growth processes and eco-environment qualities were observed in dryland regions. Studies showed that drylands will accelerate their expansion by 11% to 23% by the end of the 21st century, compared to the 1961–1990 baseline under different scenarios [17], while drylands in China expanded by 8.3% in 1980–2015 based on aridity index [18]. However, there is conflicting evidence over whether drylands will shrink or expand when using different indicators under warming scenarios [19]. Although previous studies showed drylands in northern China and Central Asia significantly increased [20,21], several recent studies observed greening over many drylands [22,23] and decreased desertification of 86,704 km² in 1992–2015 in northern China due to the human protection and the decrease of wind speed [24]. These conflicting results implied the complexity of desertification and the necessity of understanding the variation patterns of desert environments [25].

It is very challenging to quantify how dryland responses to global environmental change because of the complex and dynamic feedbacks between the environment and ecosystem functions [2]. In the past decades, global climate has undergone unprecedented changes. These frequent climatic dynamics have profoundly affected dryland ecosystems, leading to uncertainties of environment changes in desert regions [26]. Among these climatic factors, precipitation and temperature are two main critical ones in controlling vegetation growth [15,21]. It is noted that the effects of climate on vegetation varied at different spatial and temporal scales [21], and small increases of precipitation could lead to a significant growth of vegetation in arid regions [27]. Moreover, vegetation coverage in northern hemisphere have been significantly changed due to global warming [28].

In addition, human activities, such as ecological conservation programs, also significantly affect vegetation activities [9]. Human activities often have a dual effect on vegetation growth by revealing land-use changes. For example, urbanization and excessive reclamation will have negative effects on vegetation activities [29], while ecological conservation projects will promote vegetation restoration [30]. To hinder the development of desertification, Chinese government has implemented many ecological restoration projects and

policies since the end of 1970s: e.g., the Three-North Shelter Forest Program (TNSFP), Grain for Green Project (GGP), Natural Forest Protection Program (NFPP), the Shelterbelt Forestry Project of the Yangtze/Pearl River Basin, and the Beijing-Tianjin Sandstorm Source Control Project, etc. These projects greatly promoted the vegetation recovery of eco-fragile regions. Evaluating the effects of these policies will help to solve the environmental problems in these areas. Vegetation changes in desertified regions that are experiencing intensified human activities are often affected by both climatic and anthropogenic factors. Therefore, it is critical to distinguish the relative contribution of these factors.

The Kubuqi desert is the seventh-largest desert in China and is also the nearest desert to Beijing. Therefore, the ecological conservation of Kubuqi is very important, since it affects the air pollution and ecological security in Inner Mongolia, Beijing, and other surrounding regions [31,32]. The core regions of Kubuqi desert were located in the Hangjin Banner, in which the desert accounts for approximately 52% of the whole Banner. To reduce the desertification and dust storms, the government implemented lots of ecological conservation activities, such as the TNSFP and GGP, to work on the extremely fragile environment in this region. Nowadays, Kubuqi has turned out to be one of the most successful areas of ecological restoration in China. It has been known as the “Kubuqi Model” and been recommended as one of the successful environmental management experiences for preventing desertification in China by the United Nations Environment Programme (UNEP) and the United Nations Convention to Combat Desertification (UNCCD) [30]. Studies showed that China is one of the few countries where vegetation has been significantly greening since the 2000s due to ecological projects [33,34]. However, it remains controversial on the relative contribution of the policies driving recovery efforts to vegetation restoration. For example, it is reported that ecological projects had failed to reverse desertification in northern China during the early stage of afforestation [35]. A study also illustrated that the effect of human activities on vegetation greening was far less than climate at a regional scale on the Mongolian Plateau [36]. The quantitative contributions of climatic factors and anthropogenic activities to the dynamics of vegetation activities are still poorly understood. Therefore, a systematic assessment of environmental changes and their drivers in Kubuqi is urgently needed.

Therefore, vegetation dynamics in the core regions of the Kubuqi Desert were examined, and their responses to climate change and human activities were quantified using long-term remote-sensing datasets from 1986 to 2020. The aims of this study are: (1) to characterize the spatiotemporal patterns of vegetation activity dynamic in the study area and (2) to quantify the relative contribution of climate changes and human activities to vegetation dynamics by using multiple linear regression and residuals trend methods. Our results improved the understanding of the interactions among vegetation dynamics and climate and ecological policies and provided references for environmental protection and sustainable development in other ecologically fragile areas.

2. Materials and Methods

2.1. Study Area

The Kubuqi desert is located in the southwest of Inner Mongolia in China and is also located on the northern Ordos Plateau and on the southern bank of the Yellow River. The core region of the Kubuqi desert is located in the central and northern parts of the Hangjin Banner, whose area is approximately 9.87×10^3 km², accounting for 52.2% of the whole area of the Hangjin Banner (Figure 1). The Hangjin Banner covers an area about 1.89×10^4 km² at elevations from about 1000 m to 1619 m. The elevation decreases from southeast to northwest. The lowest regions are close to the south bank of the Yellow River. The Hangjin Banner is part of the arid and semiarid regions of northwestern China, which has a temperate continental climate that is dry, with little rain. The annual mean temperature and annual cumulated precipitation in the region were 6.8 °C and 245 mm, and the annual evaporation is 2720 mm [37]. Most of the precipitation was concentrated in the summer, from June to August, with high interannual variability [38]. Because of

the extremely arid climate, the environment of the Hangjin Banner is very fragile and easily suffers from desertification and sandstorms. The formidable nature environment and inappropriate human activities (e.g., over-cultivation, grazing, and logging [39,40]) resulted in the serious degradation of the environment in the region from the 1980s to the early 2000s, such as through soil erosion and desertification, grassland degradation, and soil salinization. Recently, the environment of the area has also undergone complex changes due to urban expansion, the development of mineral resources, and agriculture and land-use changes [39].

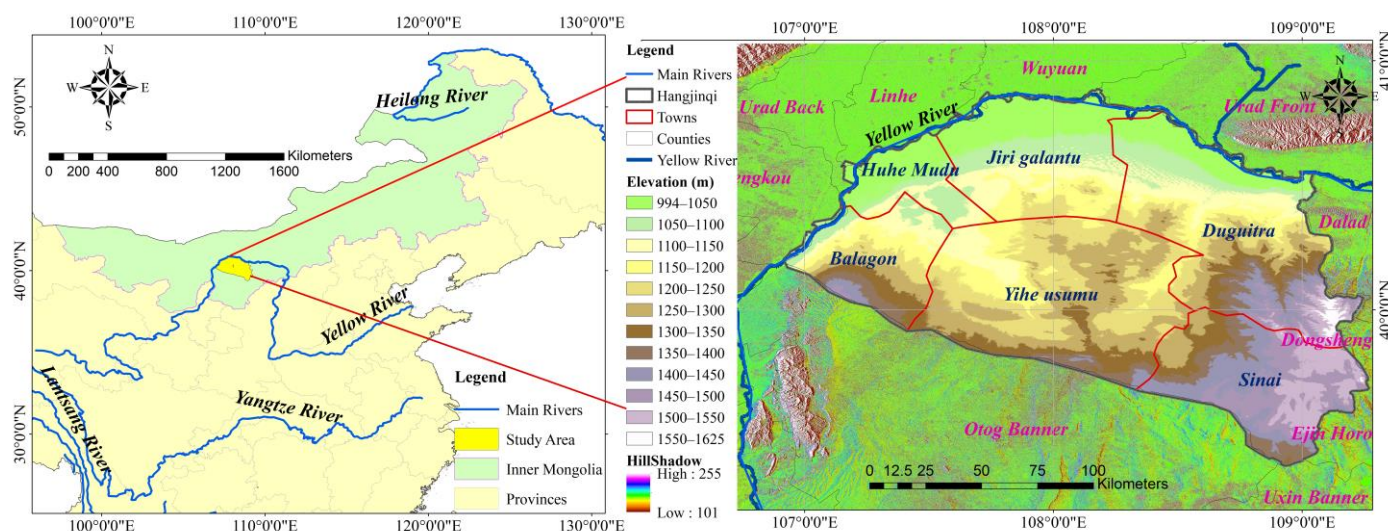


Figure 1. Locations and elevation distribution in the Hangjin Banner, the core regions of the Kubuqi Desert.

2.2. Data Sources and Preprocessing

The FVC is an important parameter for indicating environment quality and vegetation changes. In this study, we analyzed the environment dynamic changes in the Hangjin Banner using the time-series vegetation parameter of FVC from 1986 to 2020. We estimated the FVC using the dimidiate pixel model with Equation (1), which can maximize the vegetation information and reduce the influences of atmospheric, soil background, and vegetation types [8,16].

$$FVC = \frac{(NDVI - NDVI_s)}{(NDVI_v - NDVI_s)} \quad (1)$$

where $NDVI_v$ and $NDVI_s$ are the NDVI values in the pure vegetation pixels and bare land pixels, respectively. The range of FVC was assumed to 0–1. The upper and lower thresholds of NDVI intercepted at the 95% and 5% percentile levels of the statistical distribution of all NDVI values are viewed as $NDVI_v$ and $NDVI_s$, respectively.

The FVC estimation relies on the remote-sensing data of the NDVI, which were calculated from the 30 m-spatial-resolution Landsat images (TM, ETM+, and OLI) from 1986 to 2020. All of the above data were downloaded from the Google Earth Engine (GEE) platform. GEE is a cloud-based integration platform that can process massive amounts of data online efficiently [41,42]. In this study, we used GEE to calculate the NDVI and FVC and for the preprocessing (e.g., de-clouding of Landsat data). The maximum value composites (MVC) technique can eliminate the influences of cloud, snow, and other factors [15]. It is widely used to characterize the status of vegetation growth throughout the year. Therefore, the monthly NDVI time series were first composed based on the maximum values of the monthly Landsat datasets, then the maximum values of the monthly NDVI data during the growing season (i.e., from May to September) in each year were selected to composite the annual NDVI data.

The in situ meteorological dataset from the Hangjin Banner was available from the Climatic Data Center, National Meteorological Information Center, China Meteorological

Administration (<http://data.cma.cn/>, accessed on 1 April 2022). Furthermore, 1 km resolution of monthly mean temperature and monthly cumulated precipitation from 1986 to 2020 were obtained from (<http://www.geodata.cn/>, accessed on 1 April 2022) and were spatially downscaled from Climatic Research Unit (CRU) and WorldClim datasets [43]. To quantify the drivers of environment changes, the FVC data were also resampled to a 1 km resolution. FVC indicates the environment qualities. Following the reference of [44], we classified the FVC into five levels, i.e., very low coverage ($0 \leq \text{FVC} < 0.2$), low coverage ($0.2 \leq \text{FVC} < 0.4$), medium coverage ($0.4 \leq \text{FVC} < 0.6$), high coverage ($0.6 \leq \text{FVC} < 0.8$), and very high coverage ($0.8 \leq \text{FVC} < 1$). Similar to the previous studies [45,46], the FVC trends were classified into six types according to the FVC trend directions and statistical significance: highly significant improvement ($p < 0.01$, trend > 0), slightly significant improvement ($0.01 < p < 0.05$, trend > 0), insignificant improvement ($p > 0.05$, trend > 0), insignificant degradation ($p > 0.05$, trend < 0), highly significant degradation ($p < 0.01$, trend < 0), and slightly significant degradation ($0.01 < p < 0.05$, trend < 0).

2.3. Statistical Analysis

2.3.1. Trend Analysis of Vegetation Dynamics

The linear trend model was used to analyze the inter-annual variations of the vegetation dynamics from 1986 to 2020. The slope of the linear trend was calculated as follows:

$$\text{Slope}_{\text{FVC}} = \frac{n \sum_{i=1}^n (i \times \text{FVC}_i) - \sum_{i=1}^n i \times \sum_{i=1}^n \text{FVC}_i}{n \sum_{i=1}^n i^2 - (\sum_{i=1}^n i)^2} \quad (2)$$

where $\text{Slope}_{\text{FVC}}$ is the trend of the growing season FVC, n is the range of the time series, i is the order of years from 1 to n , and FVC_i is the growing season FVC for the i th year. $\text{Slope}_{\text{FVC}} > 0$ indicated that the annual FVC showed an increasing trend during the study period and vice versa. The F test was used to further evaluate the significance of the FVC trends over times.

2.3.2. Drivers Analysis of Vegetation Dynamics

The partial correlation analysis method was used to decompose the relationship between FVC changes and climatic factors (i.e., growing season precipitation and temperature in this study) by excluding the potential impacts of the other variables [47]. When analyzing the correlation between variables x and y , the partial correlation coefficient between x and y is performed while excluding the impacts from the remaining variable z . The exact partial correlation coefficient was determined by Equation (3) [47].

$$r_{xy,z} = \frac{r_{xy} - r_{xz}r_{yz}}{\sqrt{(1 - r_{xz}^2)(1 - r_{yz}^2)}} \quad (3)$$

where $r_{xy,z}$ is the partial correlation coefficient between x and y after excluding the effects of z . r_{xy} , r_{xz} , and r_{yz} are the correlation coefficients among the variables x , y , and z . The T test was used to analyze the significance levels of the relationship between FVC and the climatic factors.

2.3.3. Residual Analysis

It remains a challenge to separate the effect of anthropogenic and climatic factors on vegetation changes. Herein, we used the residual analysis method (RAM) to quantify the relative influences of climatic and human activities on FVC variations. The RAM assumes that, without considering other indeterministic factors, the contribution of anthropogenic factors can be identified as the residual between the observed values and the predicted values of FVC [48]. Firstly, we predicted the relationship between FVC changes and climatic variables using a multiple regression model (Equation (4)). Then, the residuals can

be indicated as the anthropogenic impact on vegetation (Equation (5)). The equations are as follows:

$$FVC_{CI} = a \times TEM + b \times PRE + c \quad (4)$$

$$FVC_{HI} = FVC_{obs} - FVC_{CI} \quad (5)$$

where FVC_{CI} is the predicted value based on multiple regression model between FVC and climatic factors, TEM and PRE represent the annual average temperature and the annual cumulated precipitation. a , b , and c are the coefficients of the regression model. FVC_{HI} is the residual representing human-induced FVC changes, and FVC_{obs} is the observed FVC value from remote-sensing images. When FVC_{HI} equals 0, it means that anthropogenic activities have no effect on the FVC. When FVC_{HI} is greater than 0, it means that anthropogenic activities have a positive effect on FVC and vice versa. The relative contributions of climatic and anthropogenic impacts on vegetation dynamics were calculated following the approach introduced in [48], which included six different scenarios (Table 1). Drivers of “only CI” or “only HI” means those whose contribution rate was 100%, and “CI dominated” or “HI dominated” represents those whose contribution rate was greater than 50%. These analyses were conducted using MATLAB 2020b and ArcGIS 10.5 software.

Table 1. Scenarios for the relative contribution of climatic and anthropogenic impacts on vegetation variations. $Slope_{obs}$, $Slope_{HI}$, and $Slope_{CI}$ presented the slope of FVC_{obs} , FVC_{HI} , and FVC_{CI} , respectively. CI and HI represent FVC variation drivers induced by climate change and human activities, respectively.

$Slope_{obs}$	Drivers	Drivers Division		Contribution Rate (%)	
		$Slope_{CI}$	$Slope_{HI}$	CI	AI
>0	CI & HI	>0	>0	$Slope_{CI}/Slope_{obs}$	$Slope_{HI}/Slope_{obs}$
	CI	>0	<0	100	0
	HI	<0	>0	0	100
<0	CI & HI	<0	<0	$Slope_{CI}/Slope_{obs}$	$Slope_{HI}/Slope_{obs}$
	CI	<0	>0	100	0
	HI	>0	<0	0	100

3. Results

3.1. Spatiotemporal Characteristics of Vegetation Dynamics

From 1986 to 2020, the annual averaged FVC in the Hangjin Banner showed an overall significantly increasing trend at a rate of 0.0011 per year, with a correlation coefficient (R) reaching 0.40 ($p < 0.05$) (Figure 2). In general, the averaged FVC increased from 0.291 in 1986 to 0.368 in 2020 and increased 26.5% during the last 35 years. The increased FVC trends suggested vegetation greening in the study area. Specifically, according to the variation trends of FVC during the study period, we observed a turning point in the FVC changes that appeared in 2001 (Figure 2). The FVC variations appeared distinct trends before and after 2001. The average annual FVC first showed an insignificantly slow degradation trend ($p > 0.05$) from 1986 to 2001 and then a dramatic greening trend from 2001 to 2020 at the rate of 0.0036 per year, with a significant correlation coefficient of 0.64 ($p < 0.01$). The vegetation activities were clearly increased in 2001–2020, shown in Figure 2, which is three times higher than the increase rate from 1986–2020.

The spatial distribution and statistics of the FVC in 1986, 2001, and 2020 are shown in Figure 3 and Table 2. The very low FVC ($FVC < 0.2$) indicates the environment qualities of the desertified land. The area proportions of very low FVC (where the core regions of the desert were located) were 53.32% in 1986, 52.48% in 2001, and 30.17% in 2020, with a decrease amount of 0.84% and 23.15% in 2001 and 2020, compared to the data in 1986 for the whole region of the Hangjin Banner. For the other types of vegetation coverage, we also found that there are no apparent increases in FVC, comparing the values in 2001 and 1986. However, there are larger proportions of increased pixels of FVC in 2020 compared with in 1986. There are approximately 67.64% of the area of FVC greening in 2020 in comparison

with FVC in 1986, while 29.24% of the area decreased and others were not changed between the two periods.

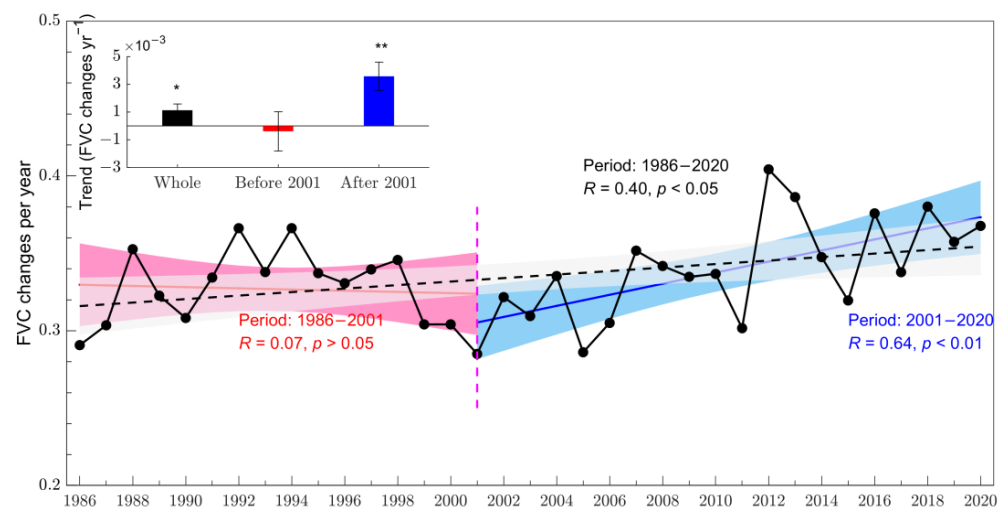


Figure 2. Temporal variations of annual FVC across the study area. The trends of FVC dynamics from 1986 to 2020 (black dotted line), 1986 to 2001 (red solid line), and 2001 to 2020 (blue solid line) were plotted. The level of statistical significance ($p < 0.05$) and ($p < 0.01$) were labeled with “*” and “**”, respectively.

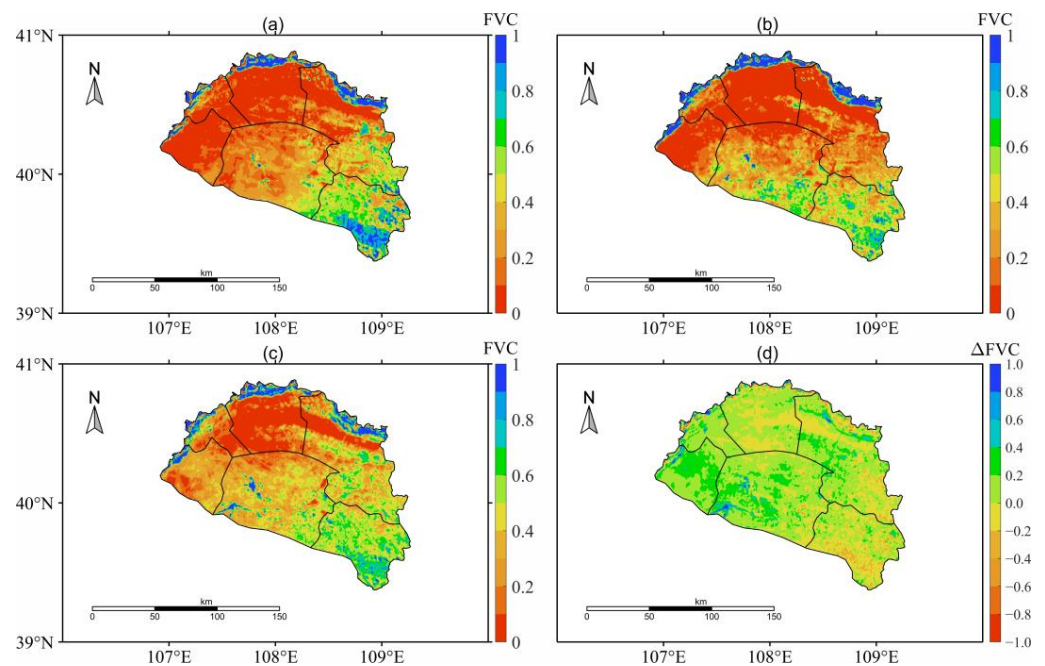


Figure 3. Spatial distribution patterns of FVC in the Hangjin Banner in 1986, 2001, and 2020. (a) FVC in 1986; (b) FVC in 2001; (c) FVC in 2020; (d) difference of FVC between 2020 and 1986.

Meanwhile, we also observed an obviously spatial heterogeneity among different regions in the study area. According to the distribution of low FVC, the desertification regions were mainly located in the towns of Jiri Galantu, Huhe Mu, Balagou, and most parts of Duguitra in 1986. There are only slight improvements in Yihe Usumu in 2001 (i.e., the very low FVC in 2001 decreased by 8.06% in comparison with 1986), as well as certain parts of Balagou that are close to Yihe Usumu in 2001, while the majority of the other regions in the desert did not experience obvious changes. On the contrary, the FVC in most regions of the study area showed clear improvements in 2020. The very low FVC areas decreased

significantly in 2020 compared to the same regions in 1986. The decreased proportion of the very low FVC areas ranged from 7.35% in Jiri Galantu to 57.40% in Balagou (Table 2). The environment qualities were obviously improved in the core regions of the Kubuqi Desert in 2020.

Table 2. The area proportions (%) of different FVC types in each town of the Hangjin Banner in 1986, 2001, and 2020. “2020–1986” represented the FVC differences between 2020 and 1986.

Year	Coverage	Jiri Galantu	Sinai	Balagon	Huhe Mudu	Duguitra	Yihe Usumu	Total Region
1986	Very low	81.69	10.28	89.72	76.47	50.68	45.45	53.32
	Low	6.89	19.60	7.26	10.20	18.60	37.21	20.32
	Medium	2.23	26.45	0.51	3.01	14.18	13.03	11.84
	High	1.58	22.58	0.31	1.91	6.59	2.92	6.40
2001	Very high	7.61	21.08	2.21	8.41	9.95	1.38	8.12
	Very low	81.86	10.08	80.15	68.10	62.11	37.39	52.48
	Low	5.06	27.47	11.07	13.51	19.38	31.39	20.47
	Medium	2.72	36.63	3.55	4.09	7.87	20.09	14.26
2020	High	1.51	16.05	1.07	1.80	3.21	7.45	5.82
	Very high	8.86	9.78	4.15	12.50	7.43	3.68	6.98
	Very low	74.34	2.42	32.32	54.37	29.20	15.35	30.17
	Low	11.26	18.14	51.13	24.95	29.57	47.86	31.78
2020–1986	Medium	4.39	44.04	11.02	6.15	21.33	28.24	22.15
	High	1.80	25.04	1.08	3.07	10.76	4.26	8.37
	Very high	8.20	10.36	4.46	11.45	9.15	4.29	7.52
	Very low	−7.35	−7.87	−57.40	−22.10	−21.48	−30.09	−23.15
2020–1986	Low	4.37	−1.45	43.87	14.76	10.97	10.64	11.46
	Medium	2.16	17.58	10.51	3.14	7.15	15.21	10.31
	High	0.22	2.45	0.77	1.17	4.17	1.34	1.97
	Very high	0.59	−10.72	2.25	3.04	−0.80	2.91	−0.59

The spatial distribution of the FVC variation trends from the entire period of 1986 to 2020 and of the periods before and after the breakpoint in 2001 are shown in Figure 4. The FVC change rates were classified into six types, and the statistic results are shown in Table 3. According to the distribution of the FVC trends in 1986–2020 (Figure 4a), there were only slight differences between the distribution map of FVC trends with significant levels of $p < 0.05$ and $p < 0.01$. Approximately 52.44% regions in the study area were greening, in which 30.05% were significantly improved according to the trend analysis (Table 3). The area proportion of the highly significantly improved pixels occupied 24.85% of the total area, while the slightly significantly improved proportion was 5.2%. The significantly improved areas were mainly distributed in the northern regions of the Hangjin Banner, which is the core region of the Kubuqi Desert, especially in areas of Duguitra and around the south bank of the Yellow River. Only 17.34% of regions were significantly degraded from 1986 to 2020. Similar to the previous result, there were contrasting patterns for the change trends between the period before 2001 and after 2001. Most regions (80.57%) in the study area were insignificantly changed in 1986–2001 (Figure 4b). There were only 7.59% and 11.84% regions that were significantly improved and degraded, respectively. However, in the 2001–2020 period, the significantly improved area was 20.98%, in which 22.12% of the regions were highly significantly improved, while the significantly degraded area was only 6.37%. Compared to the previous stage, the significant improved regions were located in most regions of the study area, mainly located in the towns of Duguitra and Yihe Usumu (Figure 4c).

Table 3. Statistic results of the FVC variation trend types (% of pixels).

Periods	Improvement			Insig-Improved	Insig-Degraded	Degradation		
	Highly Significant	Slightly Significant	Sum			Highly Significant	Slightly Significant	Sum
1986–2020	24.85	5.20	30.05	22.39	30.22	10.10	7.24	17.34
1986–2001	4.35	3.24	7.59	34.54	46.03	5.89	5.95	11.84
2001–2020	22.12	7.86	29.98	34.63	29.02	3.30	3.08	6.37

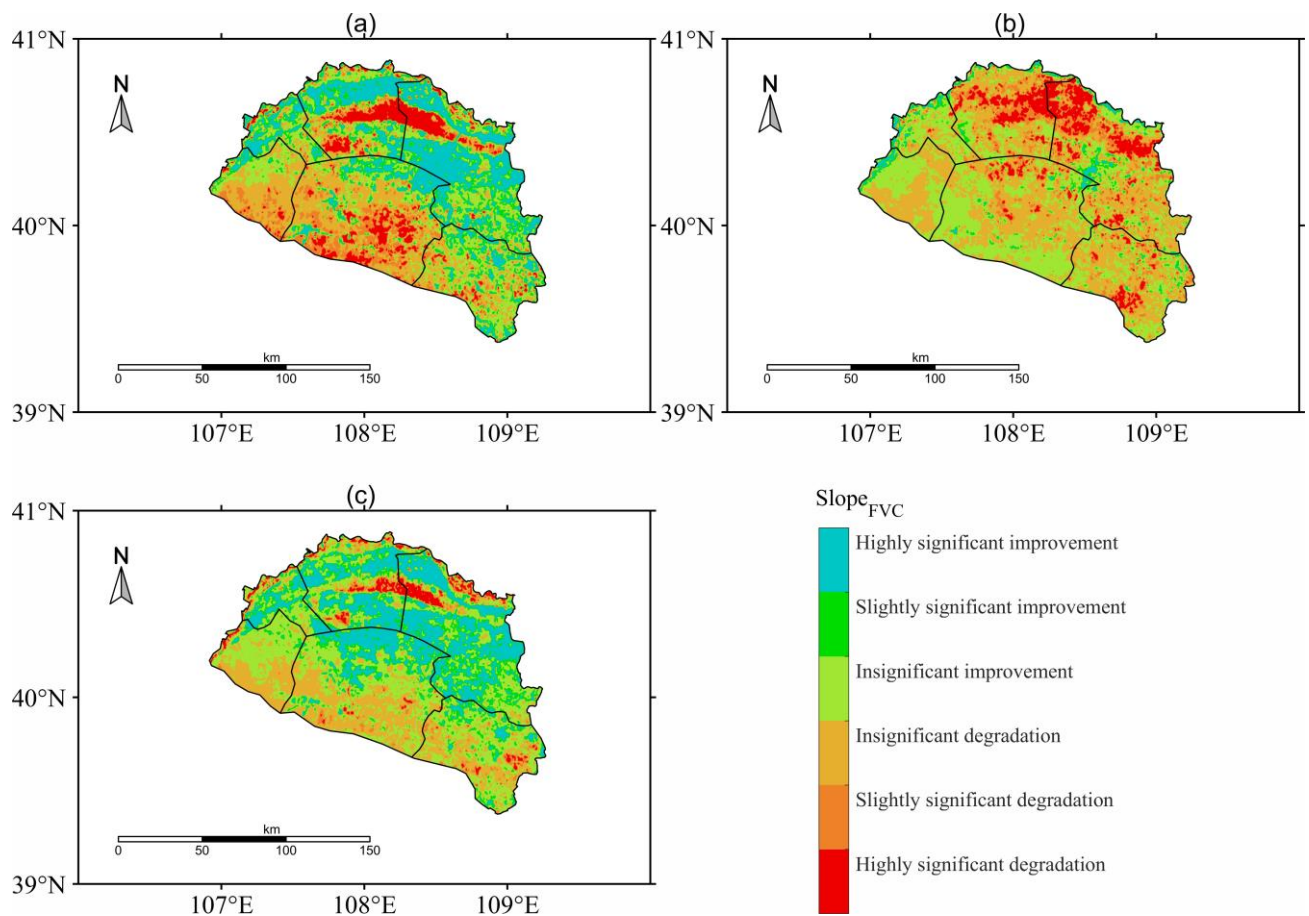


Figure 4. Spatial distribution of annual FVC change trends in the Hangjin Banner during different periods: (a) from 1986 to 2020, (b) from 1986 to 2001, and (c) from 2001 to 2020.

3.2. Relationships between Vegetation Dynamics and Climate Change

To determine the effects of climatic factors on vegetation variation, we first analyzed the relationships between the spatial averaged FVC and the meteorological data that was averaged from the in situ observations. From the whole study period, the annual cumulated precipitation appeared to exhibit a non-significantly wetting trend, with 2.26 mm/yr ($p = 0.09$). The periods before 2001 and after 2001 showed a non-significantly drying trend, with -1.19 mm/yr ($p = 0.77$), and a non-significantly wetting trend, with 5.96 mm/yr ($p = 0.57$), respectively. As shown in Figure 5a, the blue horizontal dotted line represented the average precipitation (285.89 mm) during the whole study period. We found substantial interannual variability in precipitation during the study period. The precipitation was continuously lower than the multi-yearly averaged precipitation in 1996–2000. Moreover, the correlations between FVC and precipitation were highly significant ($p < 0.01$), both in the whole period and the other two contrasting periods, with correlation coefficients of 0.75, 0.63, and 0.80, respectively (Figure 5a). The correlation coefficient after 2001 was stronger than that from before 2001.

Although there was a non-significant wetting trend for the interannual variations in precipitation, the warming trends of the mean temperature were significant ($p < 0.05$), both during the whole study period and the two distinct periods before and after 2001 (Figure 5b). The mean temperature in the Hangjin Banner showed an overall warming trend at a rate of 0.06 °C/yr, while the warming rates before and after 2001 were 0.08 °C/yr and 0.09 °C/yr, respectively. However, there was a weak correlation ($p > 0.05$) between temperature and FVC during the whole period, as well as during the two contrasting periods.

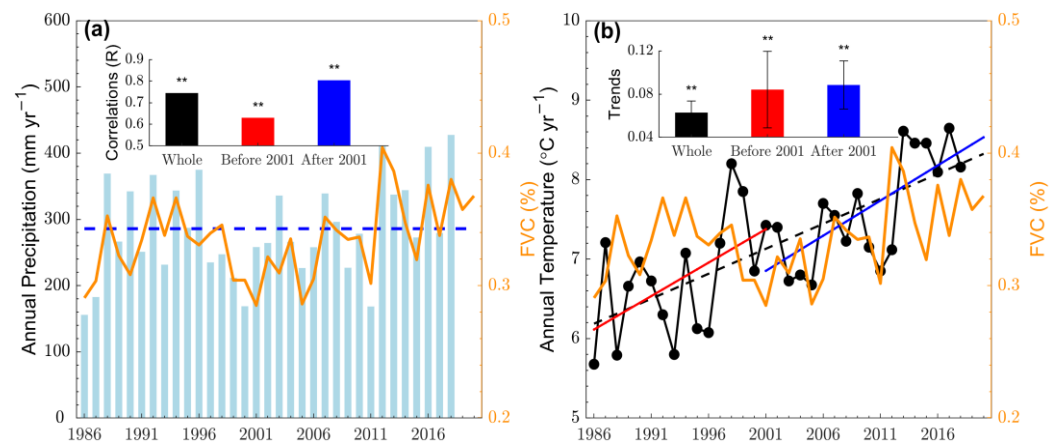


Figure 5. Interannual variation trends and correlations of climatic variables (i.e., cumulated precipitation (a), mean temperature (b)) and FVC in the study area. Climatic variables were investigated in the periods 1986–2018 (the whole period), 1986–2001 (before 2001), and 2001–2018 (after 2001). The orange curve represents the FVC variation, while the blue bar and black curve represent the annual cumulated precipitation and the annual mean temperature, respectively. The temperature variations were linearly fitted with the red solid line, blue solid line, and black dotted line during the three time periods. The level of statistical significance ($p < 0.01$) was labeled with “**”. The left sub panel represented the correlations between annual precipitation and FVC, while the right sub panel represented the change trends of annual mean temperature during the three study periods. Due to the lack of in situ meteorological data in 2019 and 2020, we only analyzed the meteorological data from 1986 to 2018.

As shown in Figure 6, the distribution patterns in annual averaged FVC were significantly spatially correlated with temperature (correlation coefficient $R = -0.35$, $p < 0.01$) and precipitation ($R = 0.46$, $p < 0.01$). The vegetation showed a greening trend from northwest to southeast, ranging from very low vegetation coverage in Balagon, Huhe Mudu, and Jiri Galantu, to medium vegetation coverage in Duguitra and Yihe Usumu, and to very high vegetation coverage in Sinai. While the temperature decreased overall from the northwest to the southeast, precipitation also showed an overall increased trend from the northwest to the southeast of the study area. The distribution patterns suggested that the core region of the desert with very low FVC was mainly correlated with very low precipitation and hot air temperature, while the distribution of very high FVC may be associated with the relatively sufficient precipitation and cool air temperature.

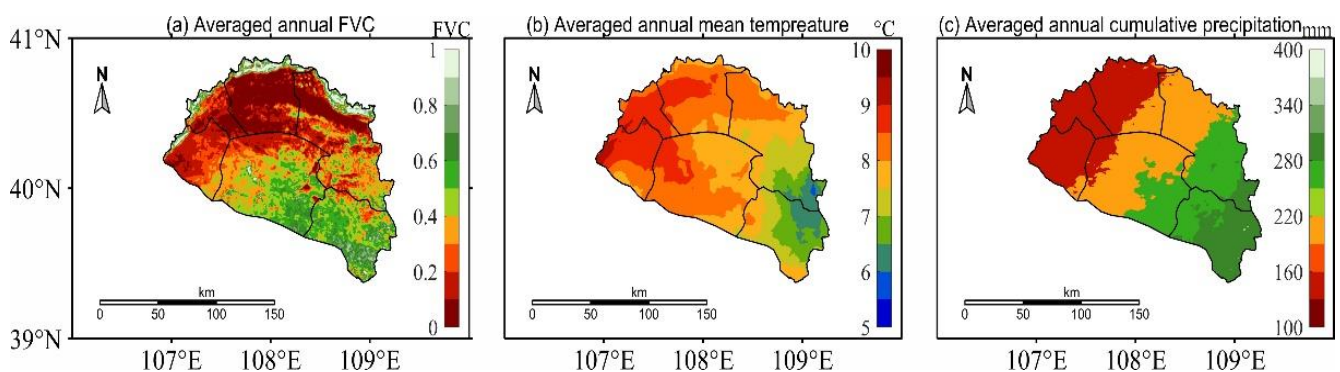


Figure 6. Spatial distributions of averaged FVC, temperature, and precipitation over the study area.

To determine the spatial variations in how climatic factors affected the vegetation variation, we further quantified the partial correlation analysis between temperature, precipitation, and FVC during the whole study period and during the two contrasting period of before 2001 and after 2001 (Figures 7–9). As shown in Figure 7, the positive pixels

of the partial correlation coefficient between temperature and FVC occupied 49.4% of the total area (Table 4). In the above regions, the significant areas ($p < 0.05$) accounted for 17.93% and were mainly distributed in areas of Duguitra and around the southern bank of the Yellow River. The area of significantly negative correlations accounted for 14.15% of the total area and was mainly distributed in the core regions of the Kubuqi Desert. The positive partial correlation coefficient between precipitation and FVC was identified in 72.31% of the study area, and 28.77% of the area passed the significance test ($p < 0.05$), mainly distributed in the southwestern region of the study area (i.e., Balagon and western Yihe Usumu). The areas with significant negative correlation accounted for only 5.15% of the total area and were mainly distributed in the core regions of the desert. Overall, the area proportion of significant correlation coefficients between precipitation and FVC was larger than that between temperature and FVC. However, the non-significant areas took up 67.92% and 66.09% of the total area, respectively, for temperature and precipitation, which suggested both of them had relative little effect on the vegetation changes in most regions of the study area.

Table 4. Area proportions (%) of a significant evaluation for the partial correlation between climate factors (Tem: temperature and Pre: precipitation) and FVC.

Time	Partial Correlation between Tem and FVC				Partial Correlation between Pre and FVC			
	Sig-Positive	Insig-Positive	Sig-Negative	Insig-Negative	Sig-Positive	Insig-Positive	Sig-Negative	Insig-Negative
1986–2020	17.93%	31.47%	14.15%	36.45%	28.77%	43.54%	5.15%	22.55%
1986–2001	5.97%	26.92%	13.57%	53.53%	18.92%	30.60%	12.51%	37.98%
2001–2020	3.19%	66.09%	0.56%	30.16%	20.02%	53.58%	2.44%	23.96%

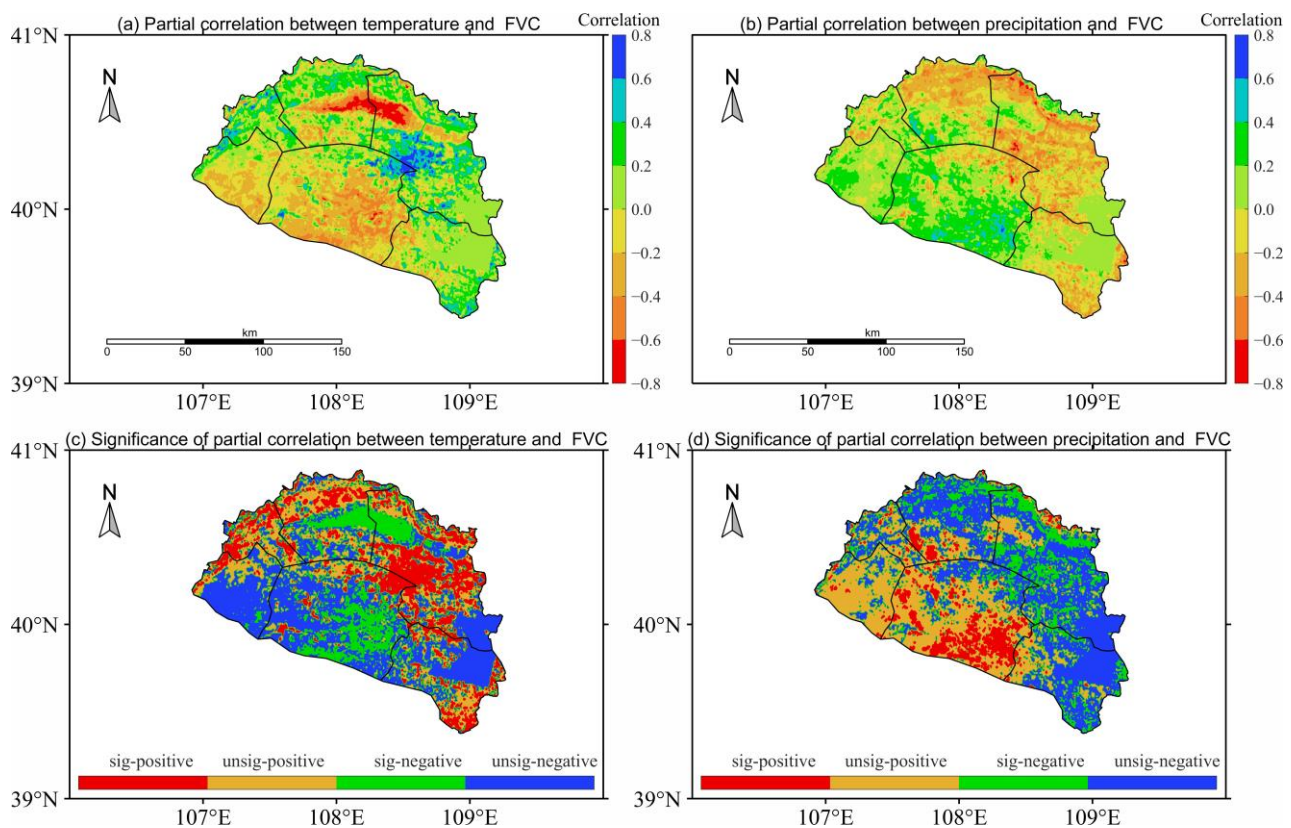


Figure 7. Partial correlations and their statistical significance between climatic factors and FVC from 1986 to 2020.

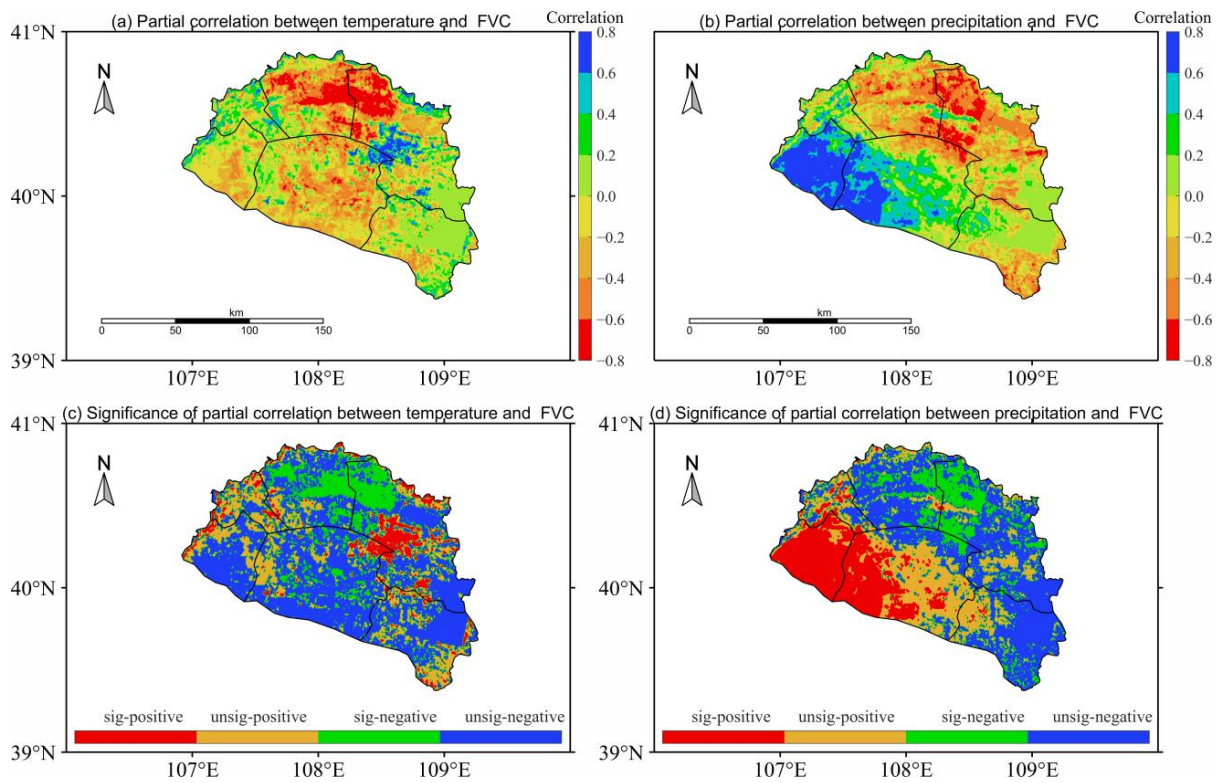


Figure 8. Partial correlations and their statistical significance between climatic factors and FVC from 1986 to 2001.

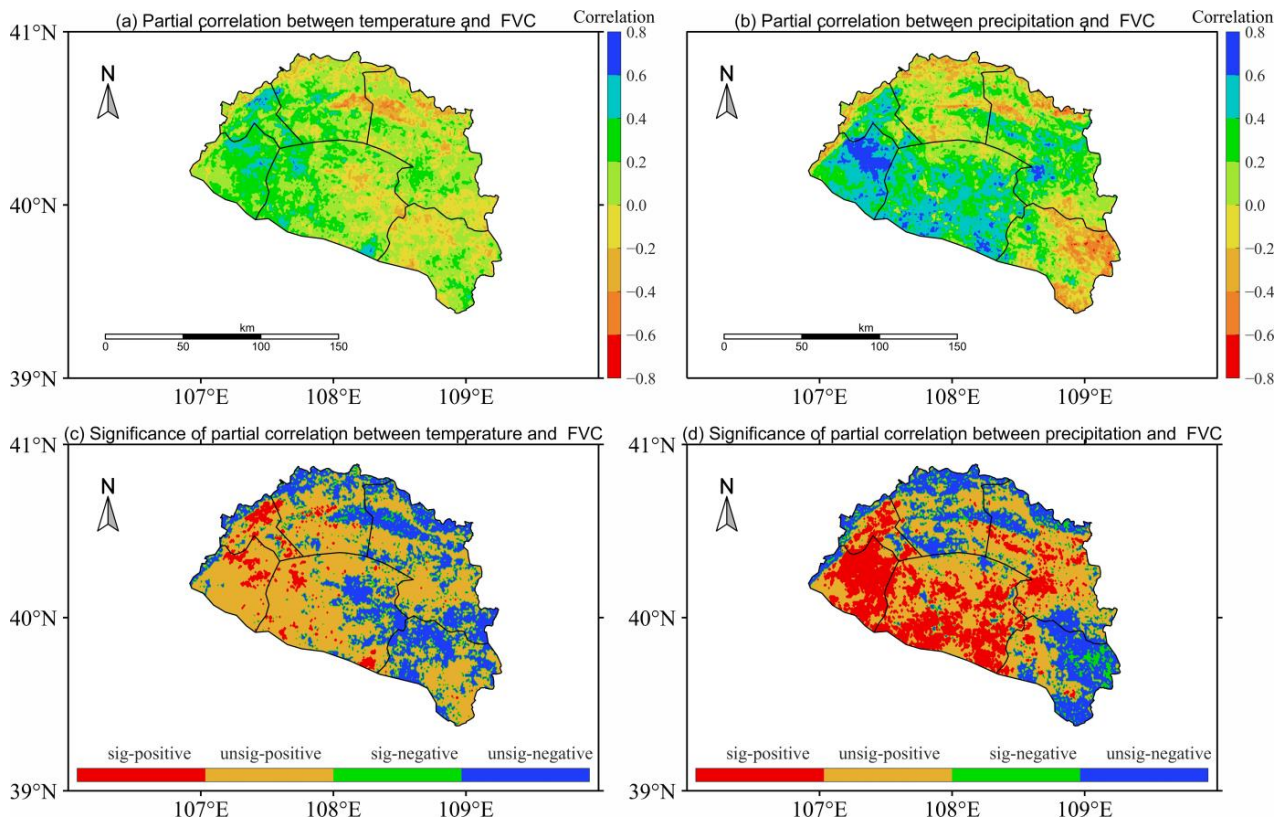


Figure 9. Partial correlations and their statistical significance between climatic factors and FVC from 2001 to 2020.

To consider the temporal variations of the effects of climatic variables on vegetation greening, we further explored the partial correlations between climatic factors and FVC during periods before and after 2001 (Figures 8 and 9). Compared to the whole period, the area proportions of the significantly positive partial correlation coefficient between climatic factors and FVC were obviously less during the 1986–2001 and 2001–2020 periods (Table 4). The significantly positive proportions of the partial correlation coefficient ($p < 0.05$) between temperature and FVC occupied only 5.97% and 3.19% of the total area during the periods before and after 2001. In the former period, the significantly positive areas were mainly distributed in the south of Duguitra, while the significantly positive regions were distributed in the latter period. On the contrary, the area proportion of the partial correlation coefficient with significantly negative values in the period before 2001 (i.e., 13.57%) were obviously greater than the significantly positive area after 2001 (less than 1%). Moreover, the area proportions with strong partial correlations ($p < 0.05$) between temperature and FVC in the later period were far less than those in the former period, which suggested a decreased influence of temperature on FVC dynamics since 2001.

In general, the partial correlation coefficient between precipitation and FVC, with significantly positive values ($p < 0.05$), was greater than that between temperature and FVC in both periods, suggesting that a stronger influence of precipitation than temperature is responsible for vegetation recovery. During the period before 2001, the area proportions of the significantly positive correlation and significantly negative correlation were 18.92% and 12.51% of the total area, respectively. In the period after 2001, the significant positive correlation area (20.02%) was clearly greater than that of the significant negative correlation (2.44%) between precipitation and FVC.

3.3. Relative Roles of Climate Change and Human Activities on Vegetation Dynamics

Both climate change and human activities are important factors affecting vegetation dynamics. In our study, the anthropogenic activities also played an essential role in the vegetation variations in the drylands of the Hangjin Banner. To investigate the potential influences of the two factors on vegetation dynamics, the relative contributions of climate change and human activities during the whole period and periods before and after 2001 were explored based on the results of the residual analysis (Figure 10). Among different time periods, the distribution patterns of the relative contribution rates of the two factors changed differently. For the relative contributions of climate change during the whole study period (Figure 10a), the contribution rates over 60% were mainly distributed in the core regions of the desert (i.e., in the central of Jiri Galantu and Duguitra) and northern Balagon, and the low contribution rate (contributions less than 20%) regions were mainly located to the southeast of Balagon. The distribution patterns of human activities induced contributions reversed compared to those of climate change. We also observed contrasting distribution patterns of the attributions of the two factors to vegetation variations during periods before and after 2001. The high values of climate-induced contributions were distributed in the northern and central regions of the Hangjin Banner, and the low values of climatic contributions were located in the southern regions of the Hangjin Banner. While only small proportions of high values of climatic contributions were mainly aggregated around the northern Balagon region, the rest of the regions experienced very low contributions from climate change. The area proportions of human-activity-induced contributions with high values occupied most regions of the study area; 11.09% and 15.48% proportions of vegetation changes were completely attributed to climate change and to human activities, respectively, and about 73.43% pixels were affected by both anthropogenic activities and climate change in the 1986–2020 period. There are about 25.33% and 19.69% pixels completely attributed to climate and to human activities, respectively, in the period before 2001, while 6.48% and 33.28% pixels were completely affected by climate and by human activities, respectively, during the last decades. The combined influenced areas of the two factors were about 54.98% and 60.25% in the periods before and after 2001, respectively.

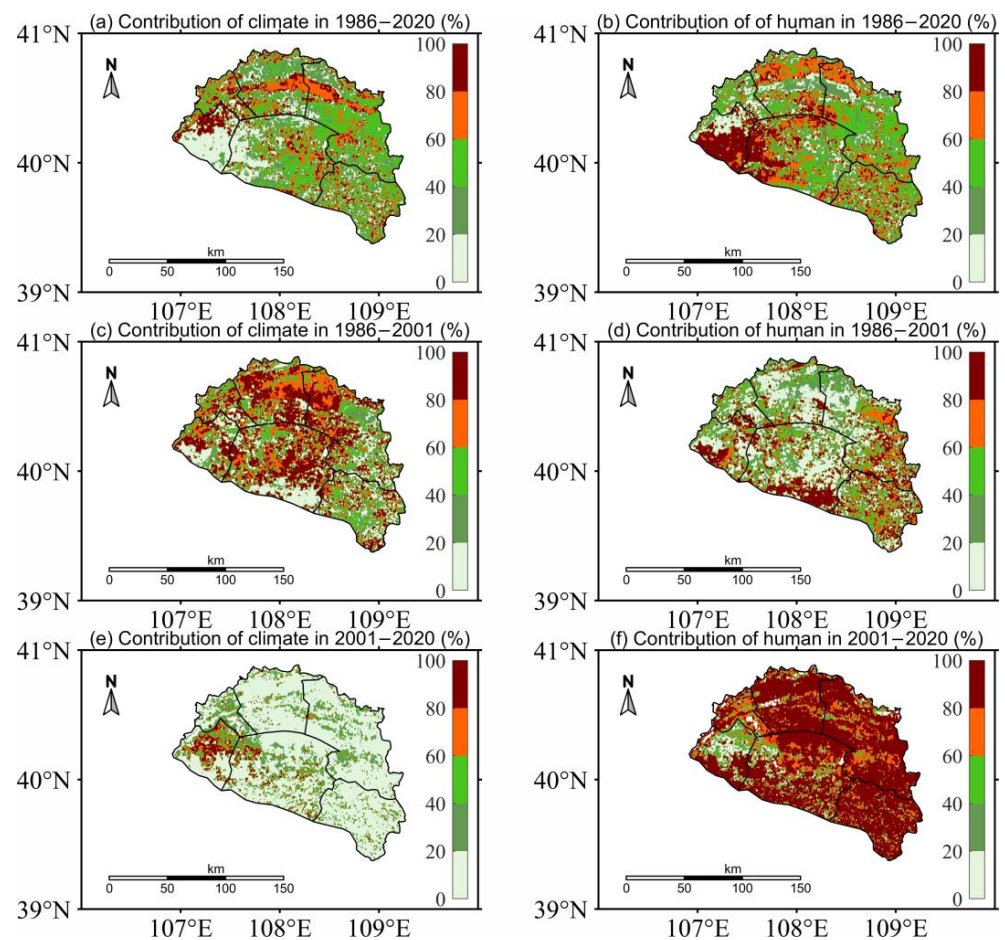


Figure 10. Spatial distribution of the relative contributions of climate change and human activities on FVC changes during 1986–2020, 1986–2001, and 2001–2020.

To compare the spatial patterns of the relative role of the climatic and anthropogenic factors in FVC changes, the FVC variation trends and relative contributions were classified into four types: CI-only, HI-only, CI-dominant, and HI-dominant. We defined a relative contribution rate of greater than 50% and less than 100% as the dominant factor and those equal to 100% as the only factor. A factor with a significantly positive contribution to FVC changes indicates that the driver played a significant role in promoting vegetation restoration and vice versa. Accordingly, the region was divided into six parts, as shown in Figure 11. The distribution of the dominant factors showed apparent spatiotemporal variability. Overall, climate change and anthropogenic activities contributed 42.15% and 57.85%, respectively, to the total vegetation variations in 1986–2020 (Table 5). The relative contribution of climate and human activities also respectively accounted for 11.38% and 20.53% in significantly promoting vegetation greening and respectively accounted for 7.86% and 6.68% in significantly restraining the vegetation improvement. In comparison, contrasting distribution patterns appeared during the periods before and after 2001. Climate and human activities contributed 58.68% and 41.32%, respectively, to the overall vegetation changes in the period before 2001, while in the period after 2001, the two factors respectively contributed 13.22% and 86.79% to the total vegetation variations (Table 5). Notably, vegetation improvements that passed the statistical significance were primarily attributed to climatic factors (4.55% of the total pixels) in 1986–2001 (only 0.88% of the total pixels were affected by anthropogenic activities) and completely attributed to anthropogenic activities (36.09% of the whole pixels) in 2001–2020. This significantly greening vegetation was mainly distributed around the core regions of the Kubuqi Desert. While the significant degraded vegetation was also primarily affected by climate change (10.57% of the whole

pixels) and human activities (4.40%) during the period before 2001, it has almost completely come from anthropogenic activities (4.66% of the whole pixels) since 2001.

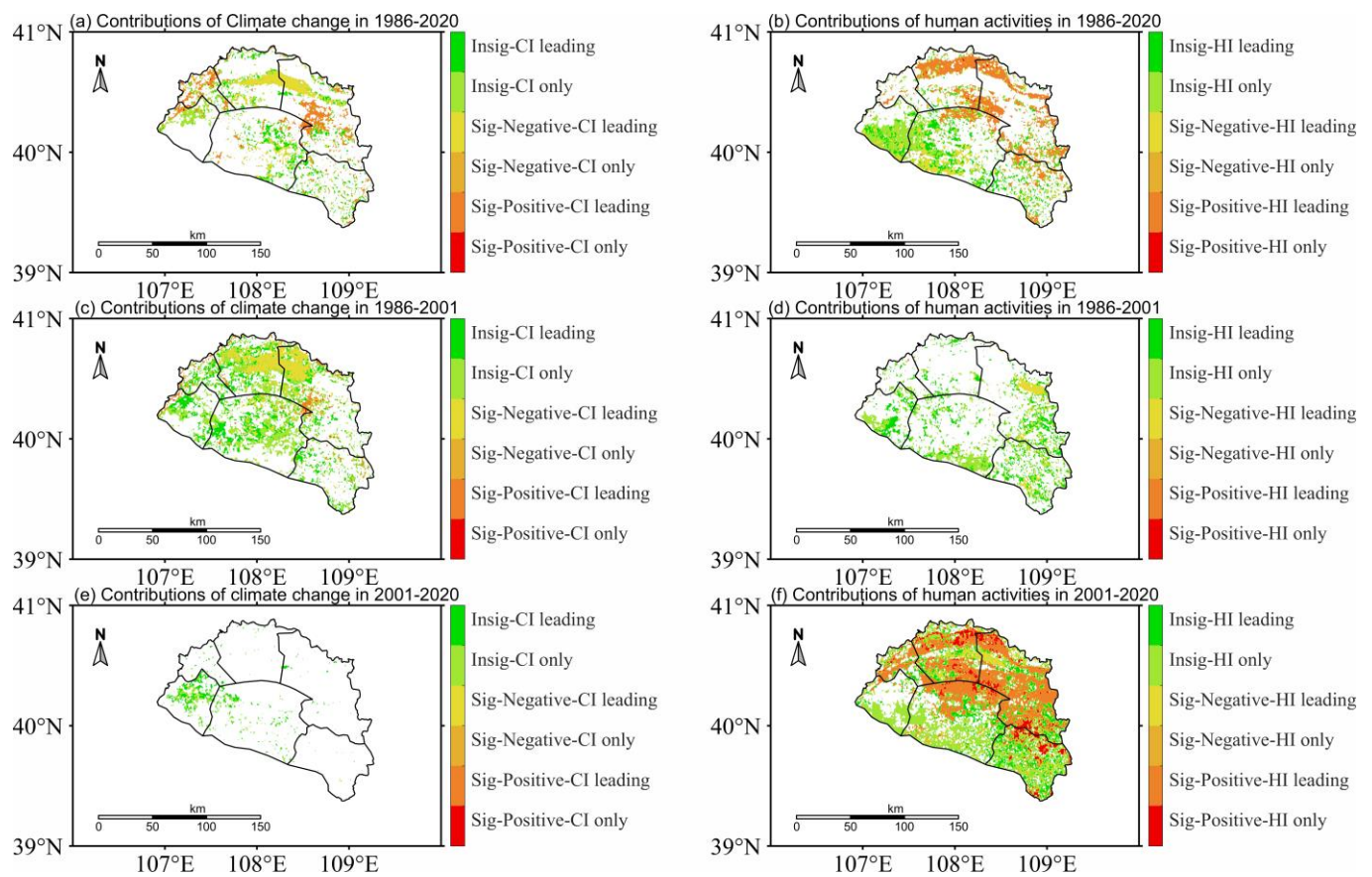


Figure 11. Spatial distribution of the effects of climate change and human activities on FVC in 1986–2020, 1986–2001, and 2001–2020. Drivers of only-CI or -HI means those whose contribution was 100%, and CI or HI leading represents those whose contribution was greater than 50%.

Table 5. Area proportions (%) of the relative contribution of climatic and anthropogenic impacts on vegetation variations. Drivers of only-CI or only-HI means those whose contribution rate was 100%, and CI-dominated or HI-dominated represents those whose contribution was greater than 50%.

Contributions	Drivers	Contribution Rate from 1986 to 2020	Contribution Rate from 1986 to 2001	Contribution Rate from 2001 to 2020
Significantly positive	Only CI	0.14%	0.31%	0%
	Only HI	0.28%	0.10%	5.22%
	CI dominated	11.24%	4.24%	0%
	HI dominated	20.25%	0.78%	30.87%
Significantly negative	Only CI	0.19%	0.18%	0%
	Only HI	0.10%	0%	0.81%
	CI dominated	7.67%	10.39%	0.01%
	HI dominated	6.58%	4.40%	3.85%
Insignificantly Changed	Only CI	10.76%	24.84%	6.48%
	Only HI	15.10%	19.59%	27.25%
	CI dominated	12.15%	18.72%	6.73%
	HI dominated	15.54%	16.45%	18.79%
Summary	Total CI	42.15%	58.68%	13.22%
	Total HI	57.85%	41.32%	86.79%

4. Discussion

4.1. Facts of Ecological Restoration over the Kubuqi Desert during the Last Three Decades

In this study, the estimated annual mean FVC values of the entire study area in 1986–2020 were 0.29–0.40, with a mean value of 0.34, which was basically consistent with the FVC mean value of 0.329 in the Pisha Sandstone area (the Hangjin Banner neighboring area) in 2000–2019 based on MODIS-EVI data [22]. Additionally, the mean FVC value (0.36) of the whole study area in 2019 was close to the mean FVC (0.35) of the Pisha Sandstone area in the same period [22]. Therefore, the FVC estimations in our study were credible and reasonable. In our study, the annual averaged FVC in the Hangjin Banner revealed an overall significant greening trend in 1986–2020. This greening phenomenon was consistent with the global greening that was reported in previous references [23,33,34]. Besides, our study also illustrated that the greening trend displayed two distinct periods separated by a turning point. The vegetation first experienced a slow variation pattern and then showed a dramatic rising trend in the subsequent period. These distinct trends in vegetation variation were similar to the other study that reported vegetation greening in Mu Us sand land [21]. Through the long-term effects of ecological conservation, such as establishing straw checkerboard barriers, artificial afforestation (Figure 12), etc., it has achieved great success in promoting the restoration of the desertified environment in the Kubuqi Desert.

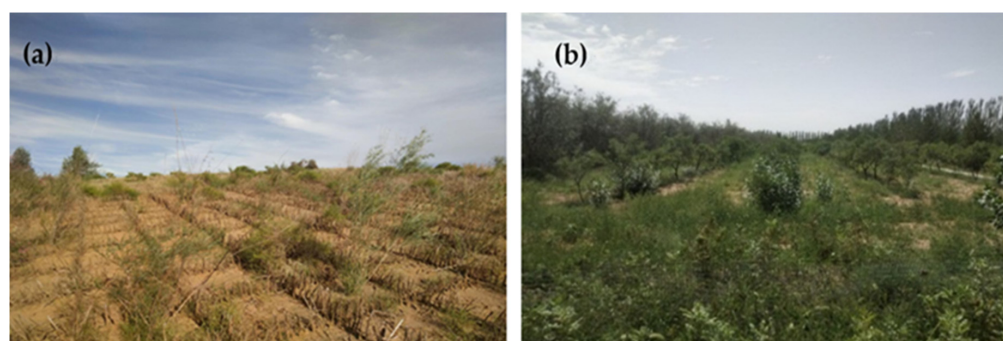


Figure 12. Photos showing ecological restoration activities in the Kubuqi Desert: (a) planted shrubs in the straw checkerboard barriers; (b) re-vegetated forestland.

4.2. Important Roles of Climatic Variables on Vegetation Variations in the Kubuqi Desert

The climate, including precipitation and temperature, have greatly influenced vegetation growth and ecological restoration. Recent studies showed a warming and wetting trend in northwestern China [49]. In our study, the interannual changes of climate revealed a significant warming and insignificant wetting trend (0.06 °C/yr, 2.26 mm/yr) over the entire period. The warming and wetting climate trend in northern China was probably attributed to the consequences of global warming [21]. Notably, there is a significant correlation between precipitation and FVC, while correlation between temperature and FVC was weak. Our studies also suggested that precipitation mainly positively correlated with vegetation greening, while the temperature mainly negatively correlated with vegetation greening. This result was reasonable since other study also supported the idea that slightly increased precipitation could significantly promote vegetation growth in drylands [27]. Moreover, there are substantial interannual fluctuations in both temperature and precipitation, with standard deviations of 0.83 °C and 72.76 mm, which significantly influenced the variability in vegetation dynamics. We found distinct vegetation variation patterns before and after the breakpoint in 2001. In the first stage, from 1986 to 2001, climate change played a dominant role (58.68%) in vegetation changes. The large fluctuations of precipitation significantly explained the vegetation dynamics in this stage. In particular, precipitation was continuously lower than normal values in 1996–2000, suggesting that a continuous water deficiency existed in these years. These drought conditions also induced a decreased trend of vegetation in the first stage. Additionally, according to the residual analysis, most areas'

vegetation dynamics cannot be well explained by the multiple linear regression model fitted by precipitation and temperature, especially in 2001–2020. This result suggested that other natural factors (e.g., radiation and evaporation) and anthropogenic factors may played an important role in controlling the spatiotemporal variations in vegetation in the study area.

4.3. Ecological Conservation Policies Dominated the Ecological Restoration over Kubuqi Desert

Besides the climatic factor forcing vegetation variations in dryland regions, human activities such as grazing, afforestation, and urbanization can also strongly affect vegetation dynamics [5,6,21]. Our study confirmed the significant greening of vegetation in the core regions of the Kubuqi Desert, which were primarily attributed to human activities rather than climate change, especially during the recent two decades. In general, the contributions of climate change and anthropogenic activities to vegetation restoration in the whole period were 42.15% and 57.85%, respectively. It is notable that the dominant role between the two factors was quite distinct in periods before and after the turning point in 2001. Climate change first led a dominant shift of 58.68% of the vegetation variation during the early period before 2001, and then anthropogenic activities contributed a leading role of 86.79% in total vegetation variation since 2001. These contrasting roles of anthropogenic activities around the turning point of 2001 were highly consistent with the history of the implementation of combating desertification and ecological conservation policies in the study area.

Due to the arid climate and improper human activities such as overgrazing and cultivation [50], the Hangjin Banner has suffered from continuous desertification in historical periods. The land degradation seriously hindered the sustainable development of economic society and the security of the eco-environment in the Kubuqi Desert. To improve the fragile environment, the Hangjin Banner was selected as the key county for conserving the eco-environment in 1998. As we summarized in Figure 13, during the last four decades, the government has implemented a lot of ecological conservation policies and projects, such as the TNSFP, the GGP, and NFPP. Although some policies were proposed before the 2000s, such as the TNSFP, which began in 1978 and has been the largest afforestation project in the world, was less effective than expected in some eco-fragile regions [35]. Our study also confirmed that the unfavorable environment could not be improved effectively by these early ecosystem restoration programs due to many factors, such as lower temperature, drier conditions, and atmospheric CO₂ concentrations, compared to that in the new century. Afforestation is difficult in these eco-fragile environments when ignoring natural ecosystem characteristics in dryland regions. A study showed that the overall tree survival rate during the afforestation project of TNSFP from 1949 to the early 2000s was only 15% in the drylands of China [35] and was not effectively implemented to promote vegetation deforestation in the early stage of the project. Therefore, the ecological policies had limited effects on vegetation restoration in the stage before 2001. This condition was also revealed by the insignificant changed area of the re-vegetated land cover (i.e., forestland and grassland) during the early stage. However, in recent decades, techniques of afforestation and experiences combating desertification have significantly improved. Through planting trees that are more suitable for arid climate in innovative ways, the tree survival rate has significantly increased now. Due to the massive “greening” effort implemented by the GGP and other similar projects since 2001, retiring and converting cropland policy and combating the desertification activities was anticipated to result in a decrease in the amount of remaining barren land and cropland, while leading to an increasing area of forestland and grassland. Finally, these ecological conservation and restoration programs effectively promoted vegetation recovery in the Kubuqi Desert. After several decades’ efforts jointed by the government (including the local armed forces), companies (e.g., Elion Resource Group Co., Ltd.), and local people, the Kubuqi Desert has been one of the most successful examples of ecological restoration and combating desertification in China [32]. Based on

the above analysis, we thus concluded that ecological policies played a leading role in vegetation greening during recent decades.

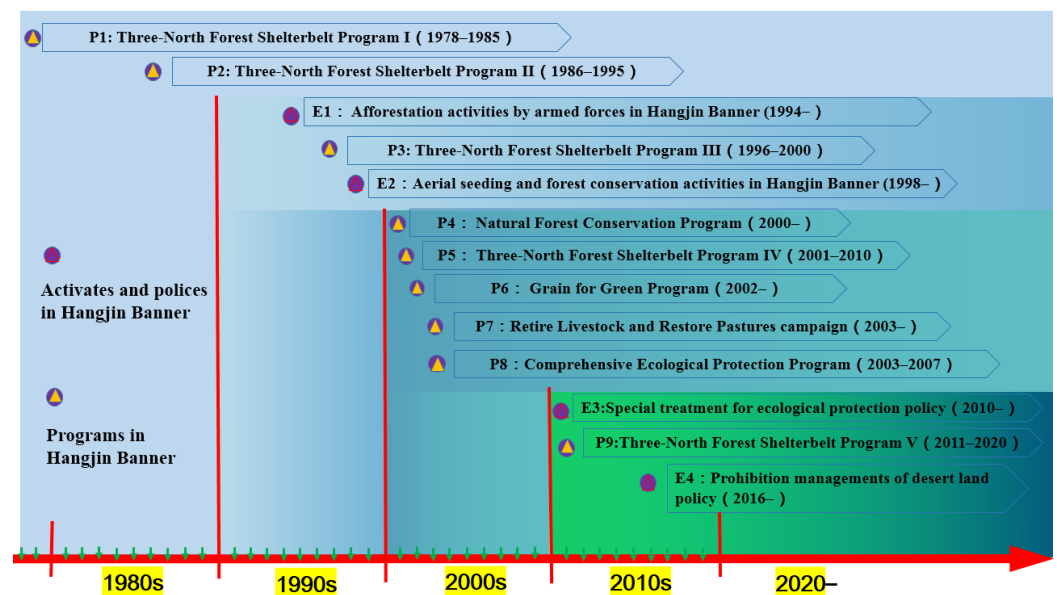


Figure 13. Timelines of the main ecological conservation and restoration programs in the Hangjin Banner over the past four decades.

4.4. Uncertainties of the Study

The research results may have uncertainties due to the influences of the uncertainties of climatic data, statistic method, and the study periods. In this study, we only selected the main climatic factors (i.e., temperature and precipitation) to construct the multi-linear regression model between vegetation dynamics and climatic variables. Although temperature and precipitation are two direct and significant factors widely selected as the driving forces of vegetation dynamics [51], other climatic factors (such as wind, radiation, etc.) also are important factors driving the variations of the vegetation growth [52]. In addition to precipitation, soil moisture can also be used to represent the water availability [3], which is commonly recognized as a primary force of vegetation growth. However, soil moisture is often measured at different depths at different sites with large variability and is typically rarely provided by the ground meteorological stations. Moreover, its relative coarse resolution also increased the uncertainties of soil moisture reanalysis dataset for analysis. Therefore, the availability of more accurate climatic data with a fine resolution has limited our understanding of the effects of different driving forces on vegetation dynamics. It is necessary for us to further study how to quantify the contribution of human activities in a more effective way.

5. Conclusions

This study quantitatively assessed the evolution processes and relative roles of climate change and human activities on ecological restoration in the core regions of the Kubuqi Desert from 1986 to 2020 based on long-term remote-sensed datasets. Our results revealed that the ecological environment generally improved significantly in the core regions of the Kubuqi Desert from 1986 to 2020, with a significant increasing rate of 0.0036/yr. Approximately 67.64% pixels of FVC in 2020 were increased in comparison with in 1986. More specific, the increasing trend experienced two contrasting variation patterns that were separated by the turning point in 2001. The vegetation first decreased slowly and non-significantly before 2001, then increased dramatically since 2001, which was three times higher than that in the entire period. The partial correlation results suggested that the relationships between vegetation dynamics and precipitation were greater than that

of temperature with large spatiotemporal variability. Both of the climatic factors cannot well-explain the variations in vegetation, suggesting the importance of anthropogenic activities. Moreover, residual analysis showed the relative role rates of the two factors varying with different time periods. Overall, climate change and anthropogenic activities contributed 42.15% and 57.85% to the total vegetation variations in 1986–2020, respectively. The relative contribution of the climate and human activities also, respectively, accounted for 11.38% and 20.53% of significantly promoting vegetation improvements and respectively accounted for 7.86% and 6.68% of significantly restraining the vegetation improvements. Similarly, the contributions of the two factors underwent two distinct patterns during the periods before and after 2001. Climate and human activities respectively accounted for 58.68% and 41.32% of the vegetation changes before 2001; after that time, these contributions contributed 13.22% and 86.79% to the total vegetation variation. These significant positive impacts of human activities on vegetation restoration were closely related to the ecological policies, which remarkably accelerate the greening of the desert in Kubuqi. These results highlighted the fact that human activities (mainly ecological policies) played a dominant role in promoting vegetation greening in Kubuqi Desert. This study emphasized that proper ecological policies could effectively improve the eco-environment of the desertified regions and prevent the desertification processes in drylands. Our study provided successful experiences with ecological conservation, which is useful for providing references for other eco-fragile areas in balancing tradeoffs between ecological protections and the sustainable development of human well-being.

Author Contributions: W.C. and H.W. conceived and designed the experiments. M.R. performed the experiments and wrote the paper. M.R. and H.W. analyzed the data. All authors contributed to the writing and editing of this paper. All authors have read and agreed to the published version of the manuscript.

Funding: This research was funded by the National Natural Science Foundation of China (grant numbers: 41871250 and 41401412) and the National Science and Technology Major Project of China's High Resolution Earth Observation System (grant no. 21-Y20B01-9001-19/22).

Data Availability Statement: Not applicable.

Acknowledgments: We thank Yong Chen, Junlei Tan, and Xufeng Wang for data collection and processing. We are very grateful to the constructive and helpful comments from three anonymous reviewers and to the availability of climate data from the China Meteorological Administration and Landsat data from the United States Geological Survey (USGS) website.

Conflicts of Interest: The authors declare no conflict of interest.

References

1. Reynolds, J.F.; Smith, D.M.; Lambin, E.F.; Turner, B.L.; Mortimore, M.; Batterbury, S.P.; Downing, T.E.; Dowlatabadi, H.; Fernández, R.J.; Herrick, J.E.; et al. Global desertification: Building a science for dryland development. *Science* **2007**, *316*, 847–851. [[CrossRef](#)] [[PubMed](#)]
2. Maestre, F.T.; Eldridge, D.J.; Soliveres, S.; Kéfi, S.; Delgado-Baquerizo, M.; Bowker, M.A.; García-Palacios, P.; Gaitán, J.; Gallardo, A.; Lázaro, R.; et al. Structure and functioning of dryland ecosystems in a changing world. *Annu. Rev. Ecol. Evol. Syst.* **2016**, *47*, 215. [[CrossRef](#)] [[PubMed](#)]
3. Wang, H.; Li, X.; Xiao, J.; Ma, M.; Tan, J.; Wang, X.; Geng, L. Carbon fluxes across alpine, oasis, and desert ecosystems in northwestern China: The importance of water availability. *Sci. Total Environ.* **2019**, *697*, 133978. [[CrossRef](#)] [[PubMed](#)]
4. Middleton, N.J.; Sternberg, T. Climate hazards in drylands: A review. *Earth Sci. Rev.* **2013**, *126*, 48–57. [[CrossRef](#)]
5. Wang, H.; Ma, M.; Geng, L. Monitoring the recent trend of aeolian desertification using Landsat TM and Landsat 8 imagery on the north-east Qinghai–Tibet Plateau in the Qinghai Lake basin. *Nat. Hazards* **2015**, *79*, 1753–1772. [[CrossRef](#)]
6. Duan, H.; Wang, T.; Xue, X.; Yan, C. Dynamic monitoring of aeolian desertification based on multiple indicators in Horqin Sandy Land, China. *Sci. Total Environ.* **2019**, *650*, 2374–2388. [[CrossRef](#)]
7. Wang, T.; Xue, X.; Zhou, L.; Guo, J. Combating aeolian desertification in northern China. *Land Degrad. Dev.* **2015**, *26*, 118–132. [[CrossRef](#)]
8. Yang, X.; Zhang, K.; Jia, B.; Ci, L. Desertification assessment in China: An overview. *J. Arid Environ.* **2005**, *63*, 517–531. [[CrossRef](#)]
9. Wang, H.; Ma, M. Impacts of climate change and anthropogenic activities on the ecological restoration of wetlands in the arid regions of China. *Energies* **2016**, *9*, 166. [[CrossRef](#)]

10. Song, W.; Mu, X.; Ruan, G.; Gao, Z.; Li, L.; Yan, G. Estimating fractional vegetation cover and the vegetation index of bare soil and highly dense vegetation with a physically based method. *Int. J. Appl. Earth Obs. Geoinf.* **2017**, *58*, 168–176. [[CrossRef](#)]
11. Song, Y.; Jin, L.; Wang, H. Vegetation changes along the Qinghai-Tibet Plateau engineering corridor since 2000 induced by climate change and human activities. *Remote Sens.* **2018**, *10*, 95. [[CrossRef](#)]
12. Geng, L.; Che, T.; Wang, X.; Wang, H. Detecting spatiotemporal changes in vegetation with the BFAST model in the Qilian Mountain region during 2000–2017. *Remote Sens.* **2019**, *11*, 103. [[CrossRef](#)]
13. Arneth, A. Climate science: Uncertain future for vegetation cover. *Nature* **2015**, *524*, 44–45. [[CrossRef](#)] [[PubMed](#)]
14. Wang, H.; Li, X.; Xiao, J.; Ma, M. Evapotranspiration components and water use efficiency from desert to alpine ecosystems in drylands. *Agric. For. Meteorol.* **2021**, *298*, 108283. [[CrossRef](#)]
15. Geng, L.; Ma, M.; Wang, X.; Yu, W.; Jia, S.; Wang, H. Comparison of eight techniques for reconstructing multi-satellite sensor time-series NDVI data sets in the Heihe river basin, China. *Remote Sens.* **2014**, *6*, 2024–2049. [[CrossRef](#)]
16. Wang, Y.; Zhang, J.; Tong, S.; Guo, E. Monitoring the trends of aeolian desertified lands based on time-series remote sensing data in the Horqin Sandy Land, China. *Catena* **2017**, *157*, 286–298. [[CrossRef](#)]
17. Huang, J.; Yu, H.; Guan, X.; Wang, G.; Guo, R. Accelerated dryland expansion under climate change. *Nat. Clim. Chang.* **2015**, *6*, 166–171. [[CrossRef](#)]
18. Abatzoglou, J.T.; Dobrowski, S.Z.; Parks, S.A.; Hegewisch, K.C. TerraClimate, a high-resolution global dataset of monthly climate and climatic water balance from 1958–2015. *Sci. Data* **2018**, *5*, 170191. [[CrossRef](#)]
19. Berg, A.; McColl, K.A. No projected global drylands expansion under greenhouse warming. *Nat. Clim. Chang.* **2021**, *11*, 331–337. [[CrossRef](#)]
20. Li, Y.; Huang, J.; Ji, M.; Ran, J. Dryland expansion in northern China from 1948 to 2008. *Adv. Atmos. Sci.* **2015**, *32*, 870–876. [[CrossRef](#)]
21. Gao, W.; Zheng, C.; Liu, X.; Lu, Y.; Chen, Y.; Wei, Y.; Ma, Y. NDVI-based vegetation dynamics and their responses to climate change and human activities from 1982 to 2020: A case study in the Mu Us Sandy Land, China. *Ecol. Indic.* **2022**, *137*, 108745. [[CrossRef](#)]
22. Wang, R.; Yan, F.; Wang, Y. Vegetation growth status and topographic effects in the pisha sandstone area of China. *Remote Sens.* **2020**, *12*, 2759. [[CrossRef](#)]
23. Pei, H.; Liu, M.; Jia, Y.; Zhang, H.; Li, Y.; Xiao, Y. The trend of vegetation greening and its drivers in the Agro-pastoral ecotone of northern China, 2000–2020. *Ecol. Indic.* **2021**, *129*, 108004. [[CrossRef](#)]
24. Chang, X.; Lu, H.Y.; Lv, N.N.; Cui, M.C.; Li, H.Y. Variation of desert and sandy field in China on the basis of remote sensing analysis and the relationship with climate change during 1992–2015. *J. Desert Res.* **2020**, *40*, 57–63.
25. Balvanera, P.; Siddique, I.; Dee, L.; Paquette, A.; Isbell, F.; Gonzalez, A.; Byrnes, J.; O'Connor, M.I.; Hungate, B.A.; Griffin, J.N. Linking biodiversity and ecosystem services: Current uncertainties and the necessary next steps. *Bioscience* **2014**, *64*, 49–57. [[CrossRef](#)]
26. Zhou, D.; Zhao, X.; Hu, H.; Shen, H.; Fang, J. Long-term vegetation changes in the four mega-sandy lands in Inner Mongolia, China. *Landscape Ecol.* **2015**, *30*, 1613–1626. [[CrossRef](#)]
27. Zhou, X.; Yamaguchi, Y.; Arjasakusuma, S. Distinguishing the vegetation dynamics induced by anthropogenic factors using vegetation optical depth and AVHRR NDVI: A cross-border study on the Mongolian Plateau. *Sci. Total Environ.* **2018**, *616*, 730–743. [[CrossRef](#)]
28. Nemani, R.R.; Keeling, C.D.; Hashimoto, H.; Jolly, W.M.; Piper, S.C.; Tucker, C.J.; Myneni, R.B.; Running, S.W. Climate-driven increases in global terrestrial net primary production from 1982 to 1999. *Science* **2003**, *300*, 1560–1563. [[CrossRef](#)]
29. Cao, S.X.; Li, C.; Shankman, D.; Wang, C.M.; Zhang, H.; Wang, X.B. Excessive reliance on afforestation in China's arid and semi-arid regions: Lessons in ecological restoration. *Earth Sci. Rev.* **2011**, *104*, 240–245. [[CrossRef](#)]
30. Zhang, F.Y.; Zhang, Z.X.; Kong, R.; Jiang, S.S.; Chen, X.; Xu, C.Y.; Tian, J.X.; Zhu, B.; Chang, J. Changes in Forest Net Primary Productivity in the Yangtze River Basin and Its Relationship with Climate Change and Human Activities. *Remote Sens.* **2019**, *11*, 1451. [[CrossRef](#)]
31. Wang, L.; Lee, X.; Schultz, N.; Chen, S.; Wei, Z.; Fu, C.; Gao, Y.; Yang, Y.; Lin, G. Response of surface temperature to afforestation in the Kubuqi Desert, Inner Mongolia. *J. Geophys. Res. Atmos.* **2018**, *123*, 948–964. [[CrossRef](#)]
32. Wang, L.; Lee, X.; Feng, D.; Fu, C.; Wei, Z.; Yang, Y.; Yin, Y.; Luo, Y.; Lin, G. Impact of large-scale afforestation on surface temperature: A case study in the Kubuqi Desert, Inner Mongolia based on the WRF model. *Forests* **2019**, *10*, 368. [[CrossRef](#)]
33. Chen, C.; Park, T.; Wang, X.; Piao, S.; Xu, B.; Chaturvedi, R.K.; Fuchs, R.; Brovkin, V.; Ciais, P.; Fensholt, R.; et al. China and India lead in greening of the world through land-use management. *Nat. Sustain.* **2019**, *2*, 122–129. [[CrossRef](#)]
34. Piao, S.; Wang, X.; Park, T.; Chen, C.; Lian, X.U.; He, Y.; Bjerke, J.W.; Chen, A.; Ciais, P.; Tømmervik, H.; et al. Characteristics, drivers and feedbacks of global greening. *Nat. Rev. Earth Env.* **2020**, *1*, 14–27. [[CrossRef](#)]
35. Cao, S.X. Why large-scale afforestation efforts in China have failed to solve the desertification problem. *Environ. Sci. Technol.* **2008**, *42*, 1826–1831. [[CrossRef](#)]
36. Miao, L.; Moore, J.C.; Zeng, F.; Lei, J.; Ding, J.; He, B.; Cui, X. Footprint of research in desertification management in China. *Land Degrad. Dev.* **2015**, *26*, 450–457. [[CrossRef](#)]
37. Liu, X.; Cai, Z.; Xu, Y.; Zheng, H.; Wang, K.; Zhang, F. Suitability Evaluation of Cultivated Land Reserved Resources in Arid Areas Based on Regional Water Balance. *Water Resour. Manag.* **2022**, *36*, 1463–1479. [[CrossRef](#)]

38. Xu, Y.; Cai, Z.; Wang, K.; Zhang, Y.; Zhang, F. Evaluation for Appropriate Tillage of Sandy Land in Arid Sandy Area Based on Limitation Factor Exclusion Method. *Land* **2022**, *11*, 807. [[CrossRef](#)]
39. Dong, X.; Chen, Z.; Wu, M.; Hu, C. Long time series of remote sensing to monitor the transformation research of Kubuqi Desert in China. *Earth Sci. Inform.* **2020**, *13*, 795–809. [[CrossRef](#)]
40. Yu, X.; Zhuo, Y.; Liu, H.; Wang, Q.; Wen, L.; Li, Z.; Liang, C.; Wang, L. Degree of desertification based on normalized landscape index of sandy lands in inner Mongolia, China. *Glob. Ecol. Conserv.* **2020**, *23*, e01132. [[CrossRef](#)]
41. Gorelick, N.; Hancher, M.; Dixon, M.; Ilyushchenko, S.; Thau, D.; Moore, R. Google Earth Engine: Planetary-scale geospatial analysis for everyone. *Remote Sens. Environ.* **2017**, *202*, 18–27. [[CrossRef](#)]
42. Wang, H.; Tan, J.; Li, X. Global NO₂ dynamics During the COVID-19 pandemic: A comparison between two waves of the coronavirus. *IEEE J. Sel. Top. Appl. Earth Obs. Remote Sens.* **2021**, *14*, 4310–4320. [[CrossRef](#)]
43. Peng, S.; Ding, Y.; Liu, W.; Li, Z. 1 km monthly temperature and precipitation dataset for China from 1901 to 2017. *Earth Syst. Sci. Data* **2019**, *11*, 1931–1946. [[CrossRef](#)]
44. Wang, Z.; Zhang, T.; Pei, C.; Zhao, X.; Li, Y.; Hu, S.; Bu, C.; Zhang, Q. Multisource Remote Sensing Monitoring and Analysis of the Driving Forces of Vegetation Restoration in the Mu Us Sandy Land. *Land* **2022**, *11*, 1553. [[CrossRef](#)]
45. Zhang, Z.; Liu, H.; Zuo, Q.; Yu, J.; Li, Y. Spatiotemporal change of fractional vegetation cover in the Yellow River Basin during 2000–2019. *Resour. Sci.* **2021**, *4*, 849–858.
46. Cai, Y.; Zhang, F.; Duan, P.; Jim, C.; Chan, N.; Shi, J.; Liu, C.; Wang, J.; Bahtebay, J.; Ma, X. Vegetation cover changes in China induced by ecological restoration-protection projects and land-use changes from 2000 to 2020. *Catena* **2022**, *217*, 106530. [[CrossRef](#)]
47. Marrelec, G.; Krainik, A.; Duffau, H.; Péligrini-Issac, M.; Lehericy, S.; Doyon, J.; Benali, H. Partial correlation for functional brain interactivity investigation in functional MRI. *Neuroimage* **2006**, *32*, 228–237. [[CrossRef](#)] [[PubMed](#)]
48. Sun, Y.; Yang, Y.; Zhang, L.; Wang, Z. The relative roles of climate variations and human activities in vegetation change in North China. *Phys. Chem. Earth* **2015**, *87*, 67–78. [[CrossRef](#)]
49. Li, B.; Chen, Y.; Chen, Z.; Xiong, H.; Lian, L. Why does precipitation in northwest China show a significant increasing trend from 1960 to 2010? *Atmos. Res.* **2016**, *167*, 275–284. [[CrossRef](#)]
50. Guo, Q.; Fu, B.; Shi, P.; Cudahy, T.; Zhang, J.; Xu, H. Satellite monitoring the spatial-temporal dynamics of desertification in response to climate change and human activities across the Ordos Plateau, China. *Remote Sens.* **2017**, *9*, 525. [[CrossRef](#)]
51. Gao, X.; Huang, X.X.; Kevin, L.; Dang, Q.W.; Wen, R.Y. Vegetation responses to climate change in the Qilian Mountain Nature Reserve, Northwest China. *Glob. Ecol. Conserv.* **2021**, *28*, e01698.
52. Zhang, Y.; Zhang, C.; Wang, Z.; Chen, Y.; Gang, C.; An, R.; Li, J. Vegetation dynamics and its driving forces from climate change and human activities in the Three-River Source Region, China from 1982 to 2012. *Sci. Total Environ.* **2016**, *563*, 210–220. [[CrossRef](#)] [[PubMed](#)]